HYDRATE CHARACTERISATION TECHNIQUES FOR PROBING THE LINK BETWEEN HYDRATE PROPERTIES AND SGA QUALITY

Ilievski, D., Whittington, B., Austin, P., Schibeci, M. and Bedell D.
A.J. Parker CRC for Hydrometallurgy, CSIRO Minerals, Bentley, Western Australia

Abstract

The literature suggests that hydrate properties are a significant determinant of the alumina properties that, in turn, determine alumina quality. It can be postulated that those hydrate properties affecting alumina quality include hydrate voidage and other hydrate structural features, such as the relative orientation between adjacent gibbsite crystallites and the location and nature of the cement binding the agglomerate.

This paper outlines techniques that have been developed or adapted to allow for the quantification of hydrate voidage (Floc Density Analyser), determination of relative changes in gibbsite crystal orientation (Raman spectroscopy and electron backscattered diffraction) and location of the cement binding agglomerated gibbsite particles (Raman spectroscopy, charge contrast and orientation contrast imaging). Existing techniques for quantification of hydrate external morphology or examination of hydrate internal structure (charge contrast imaging) are also discussed.

These techniques were used to:

(1) help establish if a particular product gibbsite particle was a single crystal or a six-fold twin.
(2) locate an "interface" region between gibbsite crystallites and show that this region was made up of crystalline gibbsite.

This suite of techniques provide the means to explore the links between alumina quality and the properties of the precursor hydrates formed under different precipitation conditions, as is being done in the AMIRA P575A "Gibbsite and Alumina Quality" project.

1. Introduction

Alumina quality is an issue of significant importance to the alumina refineries and the aluminium smelters. The survey conducted by Welch (1993) reported that the smelter operators regarded the attrition index (i.e. alumina "strength") as one of the most important SGA quality parameters.

A number of authors have noted a correlation between hydrate particle strength and SGA particle strength (e.g. Anjier and Marten, 1982; Sang, 1987; Schmidt and Taylor, 1988; Stählin et al., 1985) and their data is collated in Figure 1.

Thus, it is reasonable to postulate that understanding alumina strength will be enhanced by understanding the hydrate properties that affect hydrate strength. However, it has not been possible to quantitatively measure potentially important hydrate structural parameters such as: voidage, the relative orientation between adjacent gibbsite crystallites and the location and nature of the cement binding an agglomerate. This paper examines techniques for measuring these structural parameters, as well as techniques for characterising the external morphology and the internal structure of hydrate particles. These characterisation techniques are being used in the AMIRA P575A "Gibbsite and Alumina Quality" project that is investigating the factors affecting alumina quality.

2. Quantifying hydrate external morphology

The main problems with quantifying the external morphology of any powder materials are: (1) obtaining a representative sample, (2) processing sufficient particles for statistically significant data in a sustainable manner, (3) inferring a 3D object's structure from 2D information and (4) defining quantitative measures of morphology that are physically meaningful.

Some of the shape properties measured for alumina by the more conventional techniques reported (Siemon et al., 1988; Hsieh, 1985) include: diameter of a circle of the same area as the particle section; circularity = 4π area/perimeter^2; aspect ratio; radance (a measure of the deviation from a perfect circle obtained from Fourier analysis) and roughness (a measure of the small scale protuberances, also from Fourier analysis). Two difficulties with these measures are that they are not easily recognisable morphological features and some show poor discriminating power for hydrates and aluminas (Hsieh, 1985).

Roach and Cornell (1996) reported an image analysis expert system that supplies quantitative morphological data for hydrate particles. The design of this expert system is reported in Zaknich (1997). It works by, first, isolating the individual particles imaged by scanning electron microscopy (SEM) using neural network filters then by generating a Bayesian classifier for the particles by extracting certain features from a normalised image. These are then compared to a set of classifier values corresponding to each morphology category, which have been determined from "training data" consisting of many thousands of hydrate SEM images provided by Alcoa World Alumina. The morphology parameters generated are particle shape (classified as spherical, oblong or irregular), degree of single crystal protrusions (no, some, yes), texture (prismatic, blocky, radial, intermediate, mosaic, agglomerate), relative crystallite size (large, medium, small, fine) and degree of agglomeration (tight, medium, loose).

Our studies have found the results from this method to be acceptably repeatable, with a 95% probable error of approximately ± 10% or less in most categories. However, some of the categories were found to be strongly correlated.

Cleaver and Amal (1996) and Roach and Pearson (1999) both report on the use of light scattering to determine the

fractal dimension of hydrates. The later concluded that surface morphology information is not possible with existing equipment but shape information might be obtained.

3. Voidage measurement in hydrate agglomerates

Aggregating particles can entrap empty spaces between them. The fraction of an aggregate's volume not occupied by solid particles is called its voidage. Methods for obtaining qualitative information on hydrate voidage have been reported by Roach et al. (1988), using transmitted light microscopy on hydrate samples immersed in a liquid of the same refractive index as the hydrate (e.g. aniline) and by Roach and Cornell (1996) on the application of laser confocal microscopy and scanning electron microscopy on polished sections.

No quantitative methods for determining hydrate agglomerate voidage had been published prior to the current work. A number of potential techniques for voidage determination were evaluated, including: Laser confocal microscopy, CSIRO Floc Density Analyser, Mercury porosimetry, N_2 adsorption and pycnometry. These are briefly discussed below.

Mercury porosimetry generates a pore size distribution from the measured relationship between pressure and mercury "uptake" into the sample. However, this technique was found to be unable to differentiate between pores present within the hydrate agglomerate (intra-particle pores) and the spaces between adjacent hydrate particles (inter-particle pores). The N_2 adsorption method has the potential to determine the distribution of pores below 0.1 µm. The results suggested that the hydrates studied had few or no pores in this size range. The helium pycnometry results suggested that volume of closed pores in the hydrates studies was below the detection limit of the method.

Examination of SEM images of sectioned and polished samples can allow estimation of the extent of porosity. However, this technique suffers from the difficulties found with all microscopy techniques — obtaining representative powder samples and a representative image.

Scanning laser confocal microscopy allows the imaging of solid, intact particles in cross section. Such images could highlight the presence of pores throughout the particle. Figure 2 presents the images at various sectional depths of a laboratory-prepared hydrate particle, referred to as TC6D. This hydrate was prepared under laminar flow conditions with extremely rapid agglomeration and short cementation. The "overall" image, obtained by combining the sections, is shown in Figure 3.

Scanning laser confocal microscope images can indicate the presence of crystals — the bright sections in Figure 2 arise from suitably orientated crystallites reflecting laser light to the detector. However, the absence of a reflection in a laser confocal microscope image does not necessarily indicate the presence of a void or other specific structural information — the dark sections in Figure 2 could result from light passing through the sample or reflecting away from the detector. In this instance, the SEM images of the sectioned and polished TC6D grains indicate significant porosity (Figure 4), and some of the dark regions in Figure 2 possibly indicate voids. However, the two techniques yielded contradictory results for another laboratory prepared hydrate, referred to as CC12T7, discussed later, casting doubt on the value of scanning laser confocal microscopy as a quantitative tool for measuring hydrate agglomerate voidage.

The floc density analyser (FDA) is an instrument for determining the apparent density of aggregated particles present in flocculated suspensions (Farrow and Warren, 1989). It does this by using direct measurement of the settling velocity and particle size under conditions of Stokesian settling. Interparticle effects, which occur with some other voidage techniques, are eliminated through the use of dilute slurry solutions.

The FDA was adapted for determination of hydrate voidages; the details can be found in Bedell et al. (2000), who also showed that the voidages measured for a number of samples were qualitatively consistent with the extent of voidage apparent from SEM images of polished sections of these samples. This is illustrated for hydrate TC6D where the scanning laser confocal microscopy images (e.g. Figure 3) and the SEM images (Figure 4) indicate significant voidage, which is consistent with the voidage fraction of 0.22 ± 0.03 estimated from the FDA measurements. This is the highest voidage measured in our laboratory to date and most of the hydrate agglomerates investigated were found to be significantly less voided.

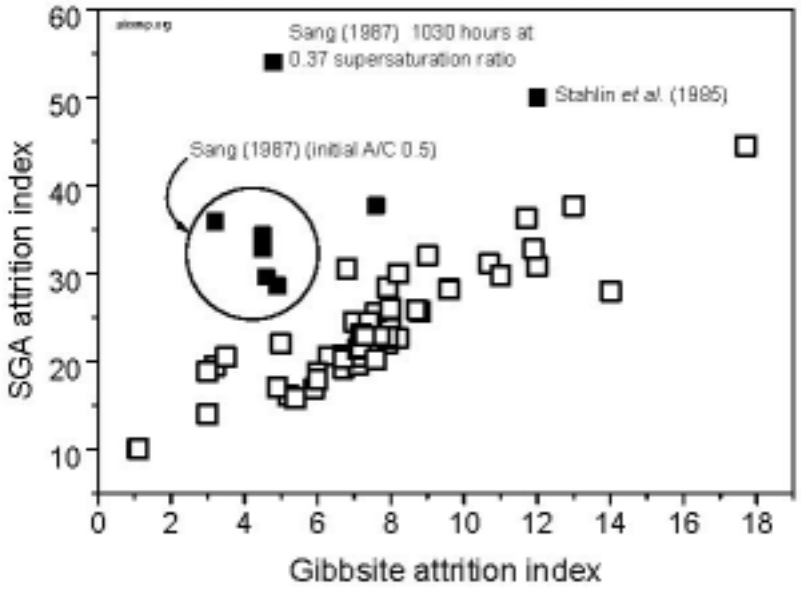

Figure 1 — Correlation between attrition indices of gibbsite and the resultant SGA (obtained from the gibbsite and SGA AI values presented in the literature: Anjier and Marten, 1982; Sang, 1987; Schmidt and Taylor, 1988; Stählin et al., 1985).

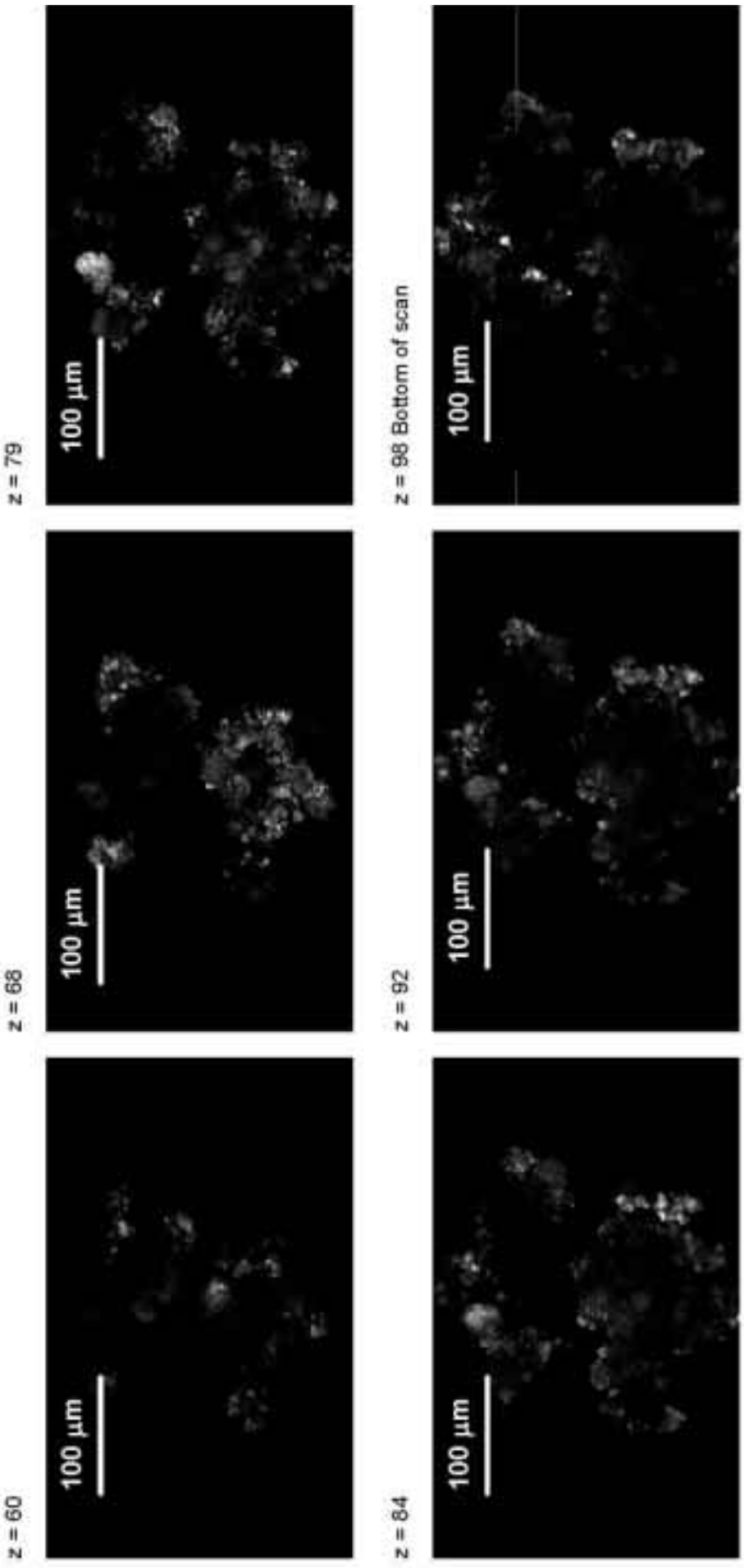

Figure 2 — Scanning laser confocal microscopy images of sections through an agglomerate from TC6D.

4. Internal structure

Griffen (1997a, b, 2000) reported that images of polished hydrate sections, obtained on the environmental scanning electron microscope (ESEM), contained bands suggestive of crystal growth structures. They refer to the method for producing such images as charge contrast imaging. Although the precise mechanism responsible for such images has not been reported, the technique's applicability to the Bayer process has been widely studied, e.g. Roach et al. (1998, 1999). Further details on this technique can be found in Baroni et al. (2000) and Watt et al. (2000).

Figure 5 illustrates charge contrast images of commercially available Alcoa C-31 hydrate and of a hydrate prepared using synthetic liquor. The images show considerable structural detail, including what could be interpreted as growth rings, discontinuities, seed and agglomerated cores. Figure 5(a) appears to show two gibbsite particles cemented by the latest layer of growth. The thickness of the latest growth layer in Figure 5(b) is consistent with that expected from the growth kinetics measured in our laboratory.

5. Crystallite orientation

Three techniques were tested for investigating differences in orientation of the gibbsite particles making up an agglomerate. These were: (1) electron back-scattered diffraction (EBSD, Kikuchi patterns), (2) orientation contrast imaging (OCI) and (3) Raman spectroscopy. All three techniques are applied to potted and polished sections of the particles.

Kikuchi lines result from the backscattered diffraction of electrons at the gibbsite surface. The positions of these Kikuchi lines depend on the crystal structure and orientation, and can therefore be used to determine absolute crystal orientation.

This technique was used to determine if a gibbsite product particle was a single crystal or resulted from "six-fold twinning" of lozenge-shaped gibbsite crystals (e.g. Sweegers et al., 1999). If the latter were the case then we would expect different crystal orientations at each of the six "lozenges" comprising the pseudo-hexagonal gibbsite basal plane (i.e. spots 1, 2, 3, 4 and 5 in Figure 6).

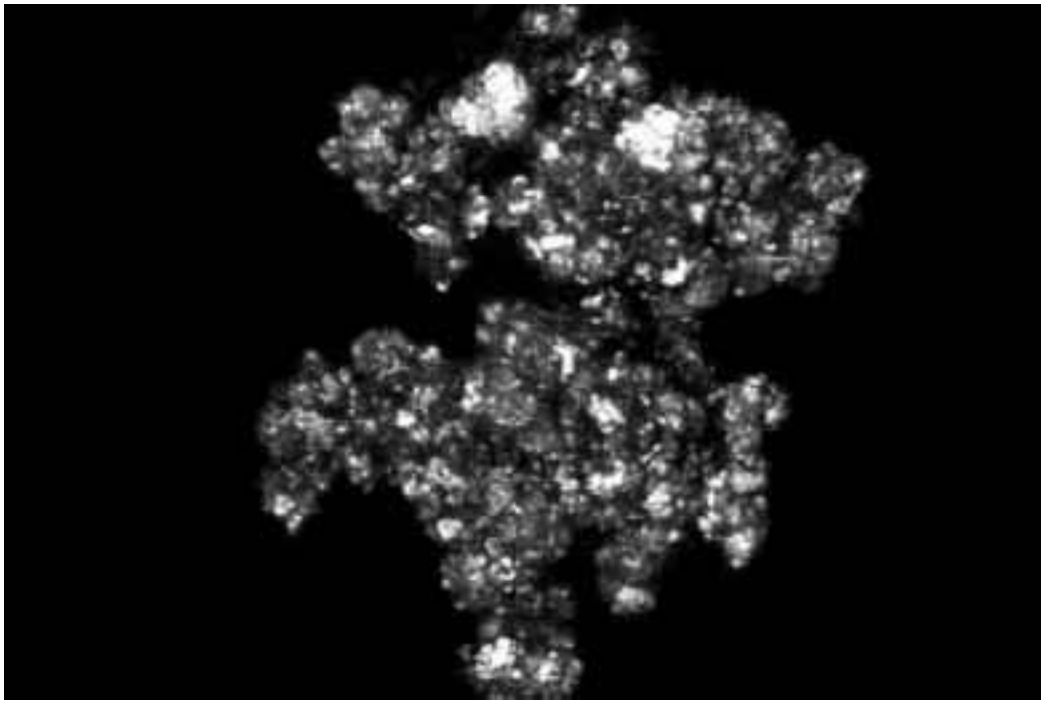

Figure 3 — Combined scanning laser confocal microscopy images of the sections from the TC6D hydrate (the software obtains an image by scanning through the "z" slices to obtain the maximum intensity value at each "x-y" pixel and then combining these to form a picture).

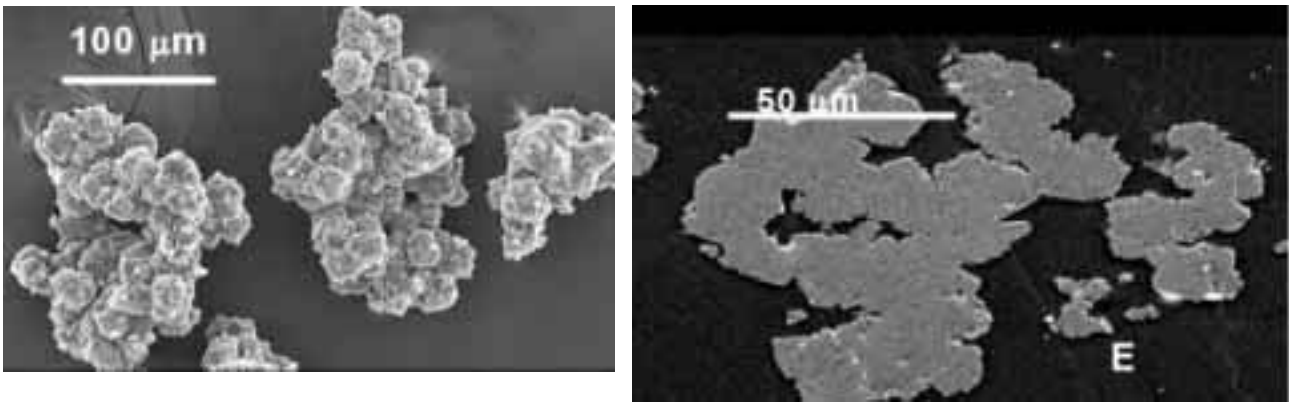

Figure 4 — SEM images of TC6D hydrate, grain-mount and sectioned and polished mount.

a) b)

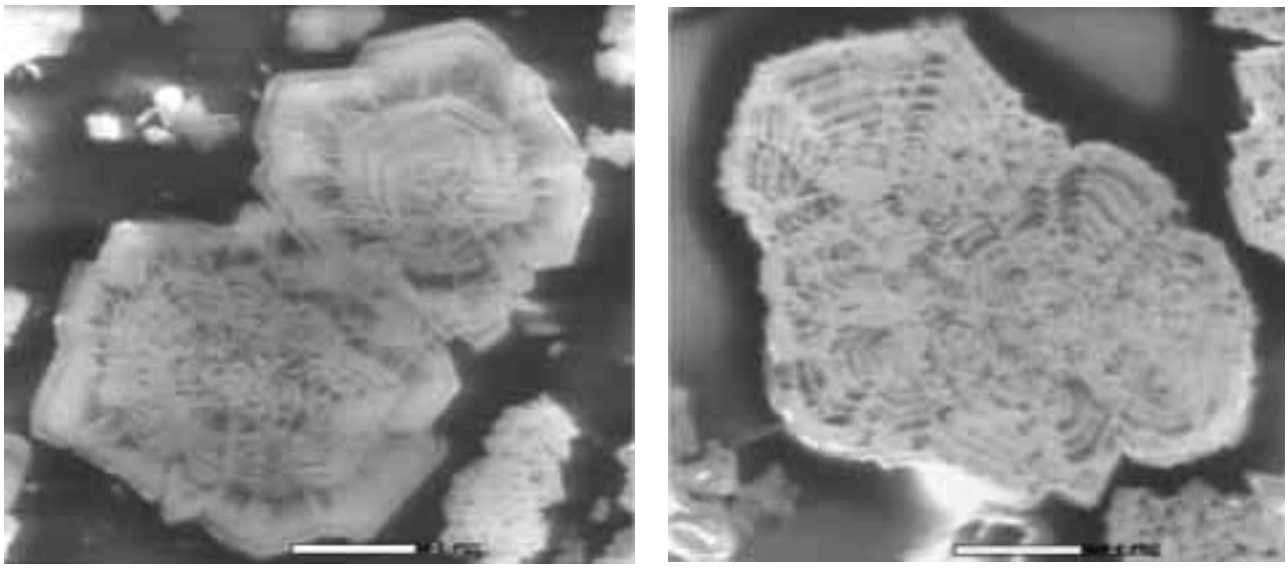

Figure 5 — Charge contrast images of a) Alcoa C-31 hydrate b) laboratory-prepared hydrate (B3-50).

Locations where EBSD images taken (orientation contrast only) Spot 1 (image 18 PL1)

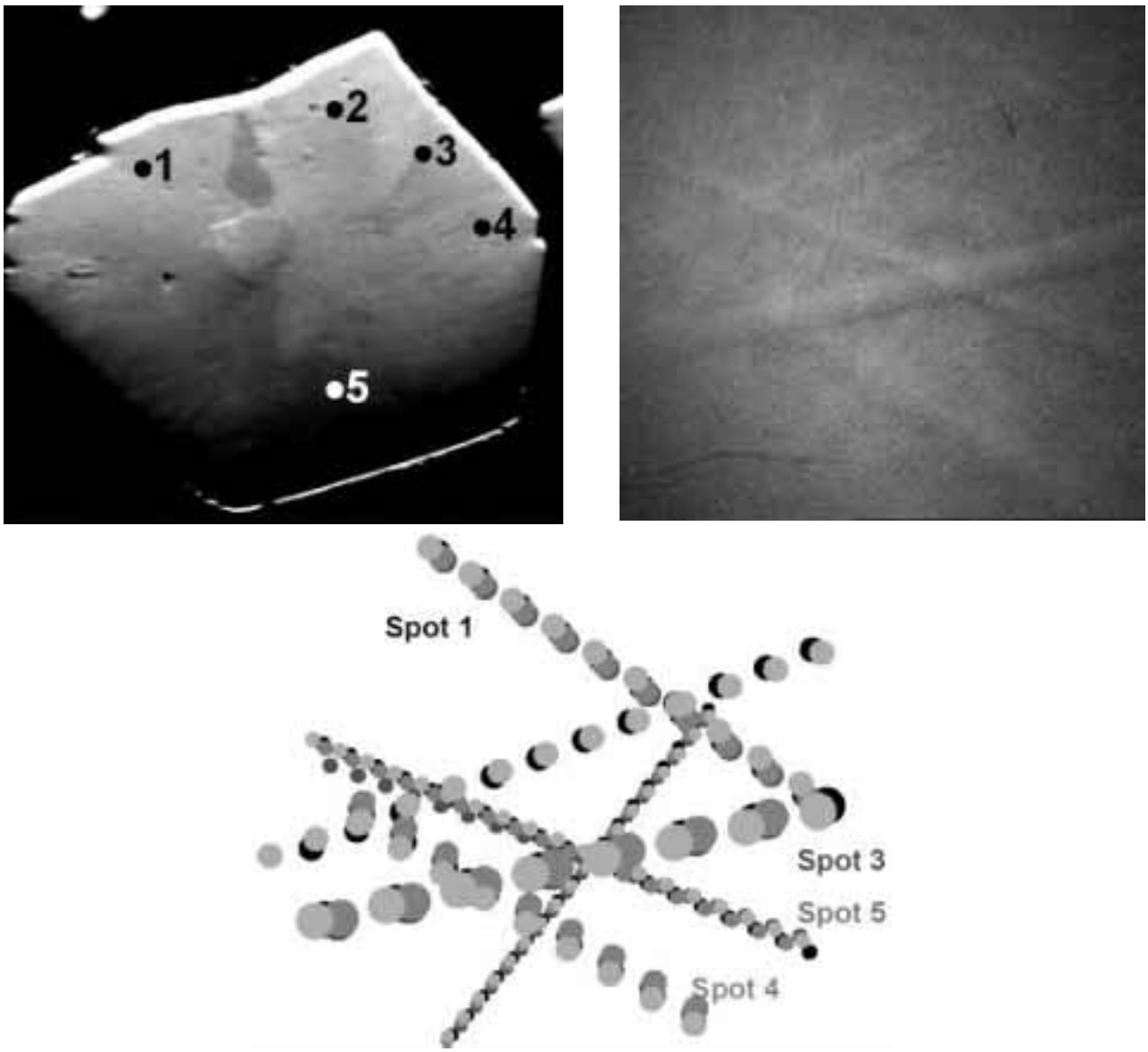

Figure 6 — Kikuchi patterns of radial gibbsite. Schematic of the overlaid Kikuchi patterns, from spots 1,3,4,5, is shown at the bottom (the use of dots is to aid comparison of the positions of the main diffraction lines in the Kikuchi patterns).

The Kikuchi pattern from spot 1, on the basal plane of a radial gibbsite, is shown in Figure 6. This pattern is represented as a schematic, which also includes representations of Kikuchi patterns obtained from spots 3, 4 and 5. The similarity of these patterns suggests no significant change in crystal orientation with location in this grain. The one exception is at spot 2, which gave a Kikuchi pattern different to the other spots. The similarity of the Kikuchi patterns obtained from spots 1, 3 and 5 indicates this particular grain does not result from six-fold twinning. However, it is difficult to reconcile the apparently different orientation observed at spot 2 with the notion that this sample is a single crystal though the lack of quantitative data regarding crystallographic parameters and crystal orientation makes it difficult to comment on the significance of this difference.

Orientation contrast imaging (OCI) is another SEM-based technique capable of yielding crystallite orientation information. However, OCI data is qualitative and relative changes in orientation within a particle are represented as variations in gray scale. A limitation of OCI is that the changes in gray scale, such as those in the OCI in Figure 6, may result from quite large or very small changes in relative orientation. This limitation requires that OCI be used in conjunction with other techniques for determining crystal orientation.

A Raman-based technique was developed at CSIRO to determine changes in gibbsite orientation. The technique works on the principle that hydroxyl groups of gibbsite are orientated in different directions (e.g. Frost et al., 1999), so that the relative areas of the hydroxyl peaks in the Raman spectrum change with gibbsite crystal/laser beam orientation. Figure 7 shows the changes observed in relative Raman peak area with orientation for a radial gibbsite "laying" along the c axis. Results from Wang and Johnson (2000), obtained subsequently, are in good agreement with our results (Figure 7).

A similar experiment, conducted using gibbsite orientated along the basal plane (e.g. as in Figure 6) also indicates an effect due to gibbsite orientation, but of different magnitude. These results suggest (i) each gibbsite orientation gives rise to a unique set of relative peak areas and (ii) Raman spectroscopy can qualitatively detect variations in relative gibbsite orientation in hydrate agglomerates.

6. Location of cement

Raman spectroscopy and OCI were used to look for changes in crystal orientation within the polycrystalline gibbsite CC12T7 prepared in the laboratory from synthetic liquor. Figure 8a and 8b present the CCI and OCI of a particular sectioned grain, and show the line along which the Raman spectra were obtained.

Figure 9 shows the variation in relative hydroxyl peak areas in the Raman spectra obtained along this line. A significant — and sudden — change in relative area of the 3533 and 3628 cm^{-1} peaks occurs at between ~37-41 µm indicating both a change in crystal orientation and that the interface between adjacent gibbsite crystallites is substantially parallel with the laser beam. Thus, the Raman spectra from the interface between ~37-41 µm should arise solely from this "interface" material.

Examination of the relative areas of these peaks suggests crystalline gibbsite is the main phase present within this "interface region". Although, in this case a detailed examination of the CCI (Figure 8a) does not unequivocally prove that the region between ~37-41 µm corresponds to cement joining crystallites (i.e. it may be a small gibbsite particle cemented between these crystallites), this example does

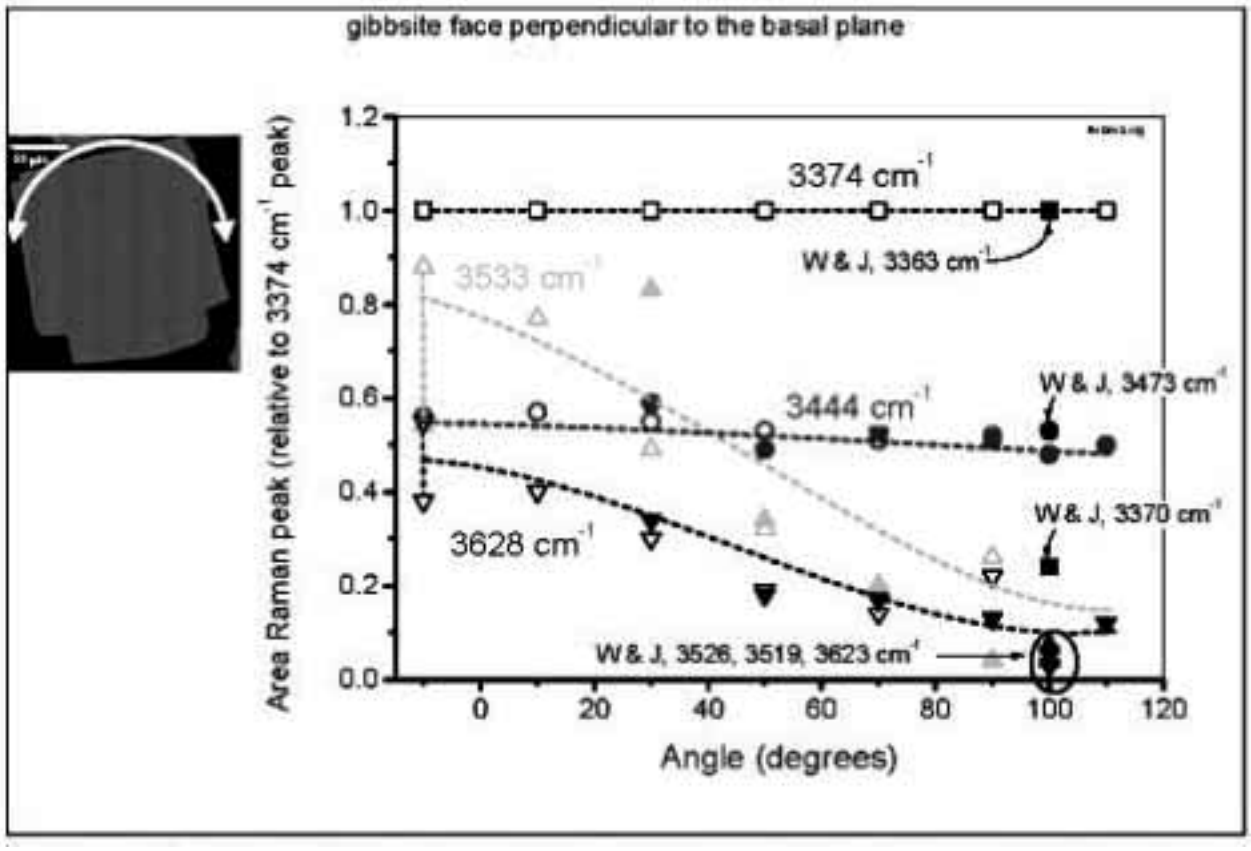

Figure 7 — Effect of crystal orientation: rotating the gibbsite crystal by a known angle about the axis shown. The data by Wang and Johnson (2000), for the a(bc')a• orientation, is included for comparison (a description of the terminology used by Wang and Johnson can be found in their paper).

illustrate how these techniques may be used to locate and investigate the cement binding the hydrate agglomerates.

7. Summary

This paper has presented various techniques for characterising hydrate structure. These are:

- an adaption of the CSIRO Floc Density Analyser for measuring agglomerate voidage;
- a Raman spectroscopy-based technique for investigating the differences in crystal orientation across a gibbsite agglomerate that can help locate cement binding the agglomerated particles;
- the use of orientation contrast imaging and charge contrast imaging to help locate the cement binding the agglomerates;
- the use of Kikuchi patterns to investigate crystal orientation
- techniques for quantifying the hydrate external morphology and internal structure.

Kikuchi patterns were used to help establish if a particular product gibbsite particle was a single crystal or a six-fold twin.

The combined application of Raman spectroscopy, orientation contrast imaging and charge contrast imaging located an "interface" region between gibbsite crystallites and showed that this region was made up of crystalline gibbsite.

Acknowledgements

The use of equipment and technical expertise provided by the following institutions is gratefully acknowledged: Curtin University School of Applied Chemistry (Peter Chapman — Raman spectroscopy), UWA Centre for Microscopy and Microanalysis (Ulrich Saydel — laser

a) b)

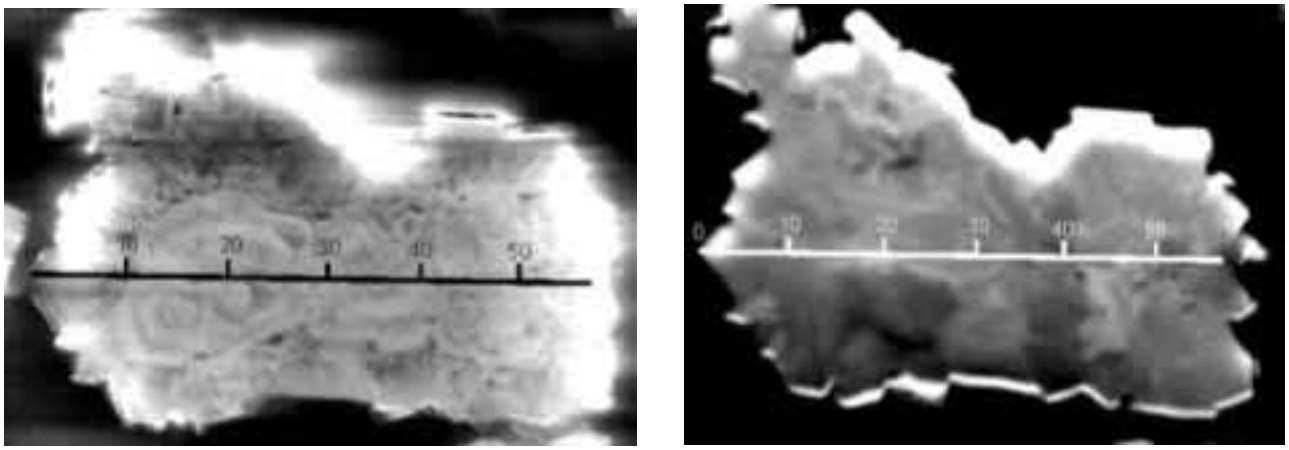

Figure 8 — Electron microscope images of CC12T7 hydrate agglomerate a) charge contrast image of sectioned and polished sample and b) orientation contrast image of the same grain examined in a).

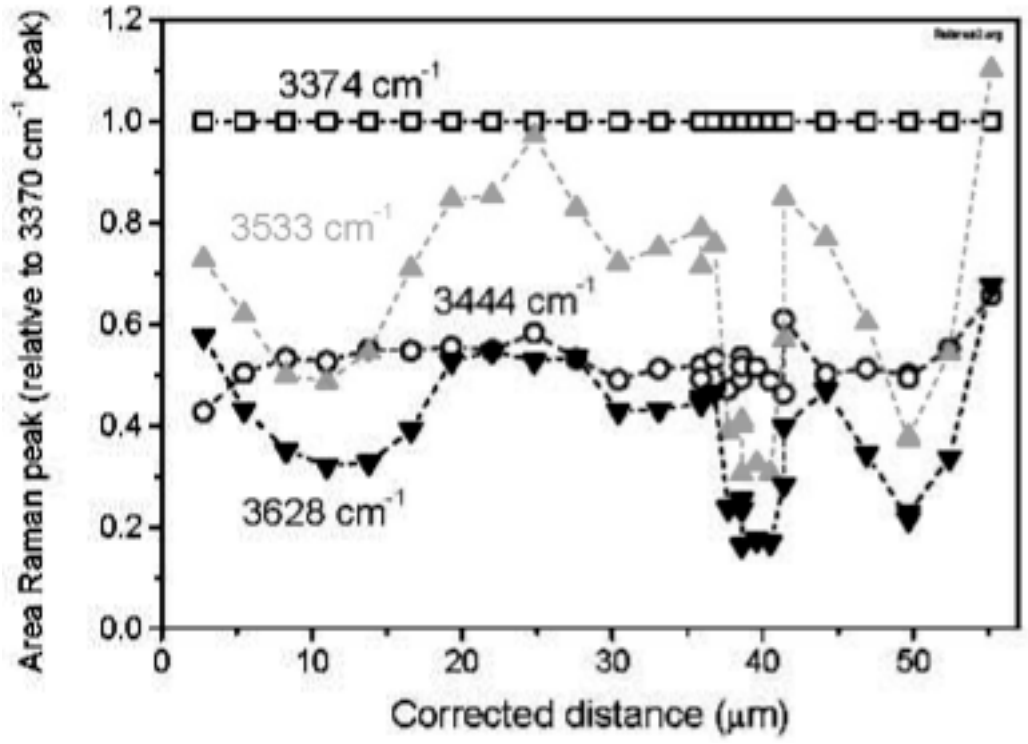

Figure 9 — Relative hydroxyl peak areas in the Raman spectra of gibbsite along the line shown in Figure 8a, b.

scanning confocal microscopy; Associate Professor Brendan Griffen, Travis Baroni and Dr James Browne — charge contrast images), Research School of Earth Sciences The Australian National University (Dr Ulrich Faul — Kikuchi patterns and orientation contrast images).

Sincere thanks go to the industrial sponsors of the AMIRA P575 project for both their financial support and their active participation throughout the project, namely: Alcoa, Worsley Alumina, QAL, Comalco, Nabalco/Alcan, Lurgi, Norsk Hydro, Billiton Aluminium, Kaiser and Pechiney. Special thanks go to Dr Steven Rosenberg of Worsley Alumina for his contributions to the project.

The authors gratefully acknowledge the support from the Australian Government's Cooperative Research Centre (CRC) program, through the AJ Parker CRC for Hydrometallurgy.

References

Anjier, J.L. and Marten, D.F.G. 1982, Particle strength of Bayer hydrate, Light Metals, pp 109–209.

Baroni, T.C., Griffen, B.J., Browne, J.R. and Lincoln, F.J. 2000, Correlation between charge contrast imaging and the distribution of some trace level impurities in gibbsite, Microscopy and Microanalysis, 6, pp 48–58.

Bedell, D., Austin, P., Whittington, B. & Ilievski, D. 2000, Voidage measurement in gibbsite agglomerates, Proceedings from Chemeca 2000, 28th Australasian Chemical Engineering Conference, Perth WA, A-3.2.

Cleaver, J. and Amal, R. 1996, Fractal analysis of alumina trihydrate, Fourth International Alumina Quality Workshop, Darwin, Australia, pp 183–189.

Frost, R.L., Kloprogge, J.T., Russell, S.C. and Szetu, J.L. 1999, Vibrational spectroscopy and dehydroxylation of aluminium (oxo)hydroxides: gibbsite, Applied Spectroscopy, 53, pp 423–434.

Farrow, J.B. and Warren, L.J. 1989, The measurement of floc density size distributions in Flocculation and Dewatering, Eds. B.M. Moudgil and B.J. Scheiner, Engineering Foundation, NY, pp 153–66.

Griffen, B.J. 1997a, Charge contrast imaging in the environmental scanning electron microscope (ESEM) — a new mechanism for the imaging of crystal structure in non-conductive materials, Australian X-ray Analytical Association Inc. (WA) and Western Australian Society for Electron Microscopy 1997 State Conference and Workshop, pp 21–23.

Griffen, B.J. 1997b, A new mechanism for the imaging of crystal structure in non-conductive materials: an application of charge induced contrast in the environmental scanning electron microscope (ESEM), Microscopy and Microanalysis, 3 (s2), pp 1997–1198.

Griffen, B.J. 2000, Charge contrast imaging of material growth and defects in environmental scanning electron microscopy — linking electron emission and cathodoluminescence, Scanning, 22, pp 234–242.

Hsieh, H.P. 1985, Morphological analysis of alumina and its trihydrate, Light Metals, pp 397–423.

Roach, G.I.D. and Cornell, J.B. 1996, Alumina and hydrate — unmasking their mysteries eight years on, Fourth International Alumina Quality Workshop, Darwin, Australia, pp 1–8.

Roach, G.I.D., Cornell, J.B. and Griffen, B.J. 1998, Gibbsite growth history — revelations of a new scanning electron microscope technique, Light Metals, pp 153–158.

Roach, G.I.D., Cornell, J.B., Griffen, B.J. and Baroni, T.C. 1999, Charge contrast imaging — application to the Bayer process, Fifth International Alumina Quality Workshop, Bunbury, Australia, pp 12–20.

Roach, G. and Pearson, N. 1999, Use of laser diffraction techniques for alumina, Fifth International Alumina Quality Workshop, Bunbury, Australia, pp 347–355.

Roach, G, I.D., Cornell, J. and Antonovsky, A. 1988 "Hydrate and alumina — unmasking their mysteries", 1st Alumina Quality Workshop, Gladstone, Australia, pp 137–148.

Sang, J.V., 1987, Factors affecting the attrition strength of alumina products, Light Metals, pp 121–127.

Schmidt, H.W. and Taylor, J.C. 1988, New developments in alumina calcination, First International Alumina Quality Workshop, Gladstone, Australia, pp 38–52.

Siemon, J.R., Gottlieb, P., Stringer, F., Hall, J.S. and Gougeon, G. 1988, The contribution of image analysis to alumina quality, First International Alumina Quality Workshop, Gladstone, Australia, pp 149–159.

Stählin, W., Bachmann, J. and Molnar, S. 1985, Alumina morphology and particle strength, Light Metals, pp 423–433.

Sweegers, C., van Enckevort, W.J.P., Meekes, H., Bennema, P., Hiralal, I.D.K. and Rijkeboer, A. 1999, The impact of twinning on the morphology of γ-$Al(OH)_3$ crystals, J. Crystal Growth, 197, pp 244–253.

Wang, S.-L. and Johnston, C.T. 2000, Assignment of the structural OH stretching bands of gibbsite, American Mineralogist, 85, pp 739–744.

Watt, G.R., Griffen, B.J. and Kinny, P.D. 2000, Charge contrast imaging of geological materials in the environmental scanning electron microscope, American Mineralogist, 85, pp 1784–1794.

Welch, B.J. 1993, Alumina quality survey, Third International Alumina Quality Workshop, Hunter Valley, Australia, pp 158–166.

Zaknich, A. 1997, Characterisation of aluminium hydroxide particles from the Bayer process using neural network and Bayesian classifiers, IEEE Trans. Neural Networks, 8, pp 919–931.